Soft Matter

PAPER

View Article Online
View Journal | View Issue

Cite this: *Soft Matter*, 2025, **21**, 9264

Dual stimuli-responsive biocompatible fluorescent hyperbranched poly(β-aminoester) for the detection of physiological temperature and pH and controlled delivery

Soumen Ghosh, Aayush Anand and Subrata Chattopadhyay *

Received 22nd June 2025,
Accepted 4th November 2025

DOI: 10.1039/d5sm00635j

rsc.li/soft-matter-journal

The sustainable synthesis of biocompatible multi-stimuli-responsive fluorescent hyperbranched polymers is an important and challenging research topic. Herein, we report the synthesis of temperature- and pH-responsive fluorescent hyperbranched poly(β-aminoester). The hyperbranched polymer structure was thoroughly analyzed *via* NMR, IR, DLS and TEM analyses, and the degree of branching was found to be 75%. Thermal analysis revealed that the polymers are thermally stable up to 180 °C and have a glass transition temperature of around −5 °C. At pH 7, the cloud point temperature (T_{cp}) was determined to be 36 °C, which is extremely close to the physiological temperature of the human body; this temperature further depends on the pH of the medium. The fluorescence intensity shows a linear dependence on temperature and pH, supporting its potential as a temperature and pH sensor. Drug release studies demonstrate the potential of the hyperbranched polymer for controlled drug delivery, showing the most sustained release under physiological conditions (36 °C and pH 7).

1. Introduction

Smart polymers are well known for their stimuli-responsive properties, which arise as a result of reversible conformational or phase changes in response to various stimuli, such as temperature, pH, light, and ions, among others.[1–7] Among the various stimuli-responsive polymers, thermoresponsive polymers are the most well studied due to their numerous applications, which include drug delivery, sensing, tissue engineering, *etc.*[8–12] These polymers show either lower critical solution temperature (LCST) or upper critical solution temperature (UCST) behavior.[6,7,13–15] Following the first report of a thermoresponsive polymer exhibiting LCST behaviour by Freeman and Rowlinson in 1960,[16] several such polymers were designed and further extended to develop dual- or multi-stimuli-responsive materials.[17–19] The most well-studied thermoresponsive polymer to date is poly(*N*-isopropylacrylamide), which shows typical LCST behaviour at ∼32 °C.[20] The thermosensitive properties of PNIPAM can be attributed to its well-known coil-to-globule transition around its LCST.[1,21] Below the LCST, the hydrophilic amide groups form hydrogen bonds with water, while above the LCST, significant dissociation of these hydrogen bonds occurs, and increased hydrophobic interaction of the isopropyl groups results in macromolecular aggregation, leading to the formation of globular structures.[1] This makes NIPAM an attractive monomer to prepare diverse thermoresponsive polymer architectures. Recent examples include poly(NIPAM)-based linear block copolymers,[22,23] hyperbranched and star polymers[24–26] and several polymer networks including hydrogels.[27,28] Here, by introducing a specific ratio of additional comonomers, the resultant thermoresponsive properties of the final polymer can be tuned. Alternatively, thermoresponsive poly(acrylamide) derivatives (PAMs), poly(2-alkyl-2-oxazoline)s (PAOxs) and poly(*N*-vinylalkylamide) have also been reported, in which the amide groups within the backbone contribute to the temperature response.[29–31] A very few examples of thermoresponsive polymers without any amide groups are also known, in which a suitable hydrophilic/hydrophobic balance results in thermoresponsive properties in PEG- and PEI-based copolymers.[32,33] Other degradable polymers, such as polyesters, do not inherently show temperature-responsive behaviour.[34] Efforts have been made to introduce the amide groups within the backbone or side chains to develop temperature-responsive polyester-based copolymers (termed as *N*-acylated PAEs).[34–36] However, to the best of our knowledge, hyperbranched fluorescent polyester-based temperature- and pH-responsive copolymers have rarely been reported.[37]

In the current work, we aimed to synthesize temperature- and pH-responsive hyperbranched fluorescent poly(β-aminoester) (existing in solution as ultrasmall molecular nanoparticles, diameter ∼10 nm), which is potentially useful for a

Department of Chemistry, Indian Institute of Technology Patna, Bihta, Patna 801106, Bihar, India. E-mail: sch@iitp.ac.in

range of applications such as temperature and pH sensing and drug delivery. Although *N*-alkylated poly(β-aminoester)s are well studied, they are rarely known to be temperature responsive.[34,38] In the literature, thermoresponsive hyperbranched polymers are less reported compared to their linear analogues. Among the existing reports in the literature, three notable approaches to prepare thermoresponsive hyperbranched polymers/nanomaterials (where the main backbone does not contain PNIPAM) can be found. The first approach involves linking temperature-responsive functionalities (such as amides/NIPAM) or polymers with the surface or branch ends of the hyperbranched polymers, with the temperature-responsive unit dictating the overall response.[2,25,39,40] The second and third approaches both involve maintaining the overall hydrophobic and hydrophilic balance. In the second approach, thermoresponsive hyperbranched polymers are prepared by introducing hydrophobic and (or) hydrophilic moieties within the polymer *via* post-polymerization modifications (by both chemical and supramolecular linking) and maintaining their suitable balance.[33,41,42] The third approach deals with developing backbone-responsive hyperbranched polymers, in which the hydrophobic/hydrophilic balance of the polymer backbone is defined by the monomers and gives rise to the thermoresponsive properties (similar to PNIPAMs).[43,44] Our current work utilizes the third approach; a hyperbranched poly(β-aminoester) is prepared by reacting hydrophobic 1,4-butanediol diacrylate with hydrophilic tris-(2-aminoethylamine) (TREN). The phase-transition temperature of the polymer is found to be 36 °C at pH 7 in water, which is one of the closest to the physiological temperature and pH. Moreover, such hyperbranched poly(β-aminoester)s are known to have nonconventional fluorescence properties. These fluorescence properties are attributed to the presence of electron-rich heteroatom functionalities (amines and esters) and their hyperbranched backbone, which promotes electron delocalization *via* through-space conjugation (TSC).[45] Therefore, a temperature- and pH-responsive phase transition is expected to influence its emission properties, and the linear correlations between fluorescence, pH and temperature make it useful as a molecular/nano thermometer. Further, the hyperbranched geometry and temperature/pH-responsive properties enable controlled delivery of encapsulated molecules under physiological conditions.

2. Results and discussion

2.1. Synthesis and characterization of hyperbranched poly(β-aminoester)

The hyperbranched poly(β-aminoester) PAE-TREN was synthesized *via* aza-Michael polyaddition reaction between 1,4-butanedioldiacrylate and tris-(2-aminoethylamine) (TREN) at room temperature in water, as presented in Scheme 1 and Table S1. After significant growth, the polymerization was quenched by high dilution, leading to the hydrolysis of the terminal acrylic ester end groups as revealed by ^{1}HNMR, FTIR and zeta-potential analysis. The occurrence of hydrolysis was supported by ^{1}H NMR (Fig. S1), as the terminal acrylate functionalities of the growing hyperbranched polymer disappear after dilution. Additionally, the linear/branched chain ratio slightly increased due to hydrolysis of a few branch ends.

The purified polymer was characterized by NMR and FTIR spectroscopy (Fig. 1). The presence of –OC**H$_2$**– methoxy protons for both the dendritic and linear units of PAE-TREN are observed at 3.5 ppm and 4.2 ppm. Two separate peaks for the methylene protons of the –C**H$_2$**– group next to the –OC**H$_2$**– groups of both the dendritic and linear unit appear at 1.5 ppm and at 1.7 ppm, respectively. A combined analysis of ^{1}H, ^{13}C (Fig. 1A and Fig. S2) and HSQC NMR (Fig. S3) revealed that the peaks at 33.1 ppm and 43.5 ppm in the ^{13}CNMR spectrum (Fig. S2) are related to the peaks at 2.3 ppm and 2.7 ppm in the ^{1}HNMR spectrum, which are attributed to the –**CH$_2$**– protons (marked as c′ and c) present in between the two consecutive amines (contributed from the TREN monomer) of the linear and dendritic units, respectively. Additionally, the peaks at 61.1 ppm and 64.9 ppm in the ^{13}C NMR spectrum are related to the peaks at 3.5 ppm and 4.2 ppm in the ^{1}HNMR spectrum, which are attributed to the –**OCH$_2$**– protons present in the linear and dendritic units, respectively. The neighboring –**CH$_2$**– groups, which appear at 1.5 ppm and at 1.7 ppm in the ^{1}HNMR spectrum, are correlated with the ^{13}CNMR peaks at 25 and 27 ppm. All the backbone peaks are assigned in Fig. 1A and Fig. S2. Hence, the

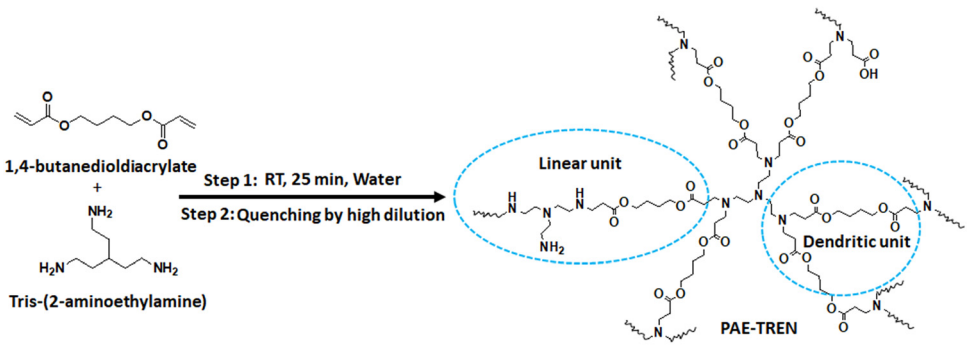

Scheme 1 Schematic depiction of the synthesis of PAE-TREN.

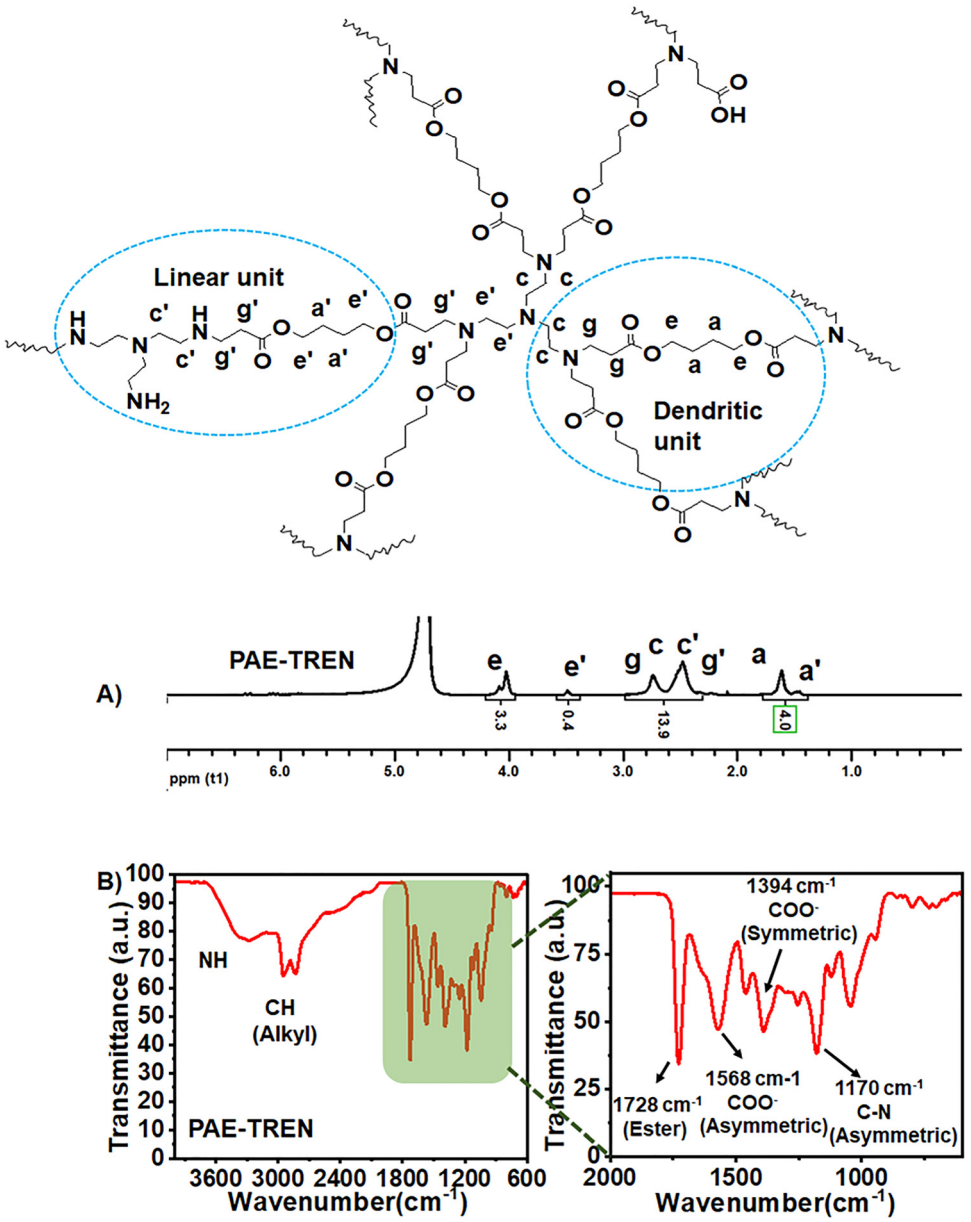

Fig. 1 (A) ^{1}H-NMR spectrum of PAE-TREN in D_2O. (B) FTIR spectrum of PAE-TREN.

presence of the characteristic peaks of the dendritic and linear units was well proven by a combination of ^{1}H, ^{13}C and HSQC NMR spectroscopy (Fig. 1A, Fig. S2, and Fig. S3).

The degree of branching (DB) of the hyperbranched poly(β-aminoester) PAE-TREN was calculated from the ^{1}HNMR spectrum using the equation DB = $2D/2D + L$, where D and L represent the dendritic and linear connectivity, respectively, as established in the literature.[46] The degree of branching for PAE-TREN was calculated to be 75%, confirming its hyperbranched structure.

The structure of PAE-TREN was further analyzed using FTIR spectroscopy (Fig. 1B). The absorption band at 1728 cm^{-1} corresponds to the presence of the –C═O (ester) functionality within the backbone. The broad absorption band at ≥3100 cm^{-1} signifies the presence of the –N–H bond in the PAE-TREN structure. The typical asymmetric stretching band of the C–N bond is distinguished at 1170 cm^{-1}. Additionally, two bands are noted at 1568 cm^{-1} and at 1394 cm^{-1}, which are characteristic of the carboxylate moiety and correspond to the asymmetric and symmetric stretching of COO^{-} (terminal/branch end), respectively.[47] The presence of the carboxylate ion was further confirmed *via* zeta-potential analysis of PAE-TREN under a range of pH values (Fig. S4 and Table S2). The negative zeta-potential values at higher pH indicate the presence of carboxylate anions generated due to the deprotonation of the carboxylic acid group, which predominates over the protonation of amine groups. On the contrary, under acidic conditions, the protonation of amine groups dominates over the

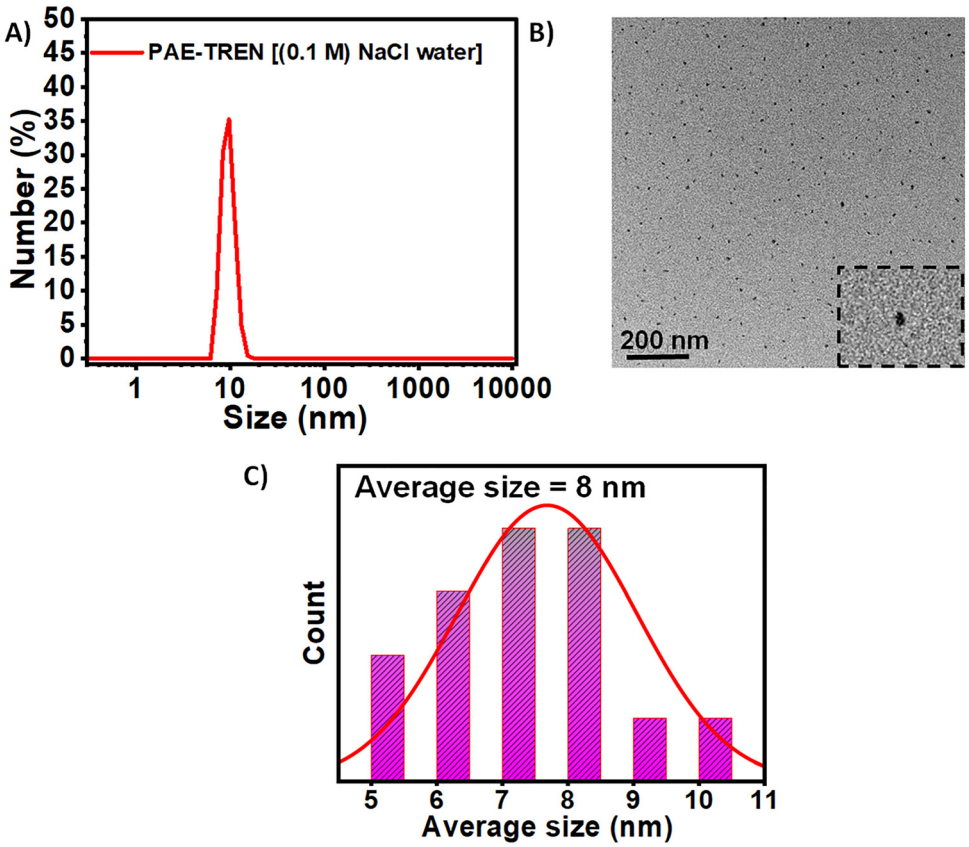

Fig. 2 (A) DLS CONTIN plot of PAE-TREN in water with 0.1 M NaCl. (B) TEM micrograph of PAE-TREN. (C) Average size distribution of PAE-TREN obtained from the TEM micrograph.

deprotonation of terminal acid groups, resulting in positive zeta potentials. The isoelectric point of the zwitterionic polymer was calculated *via* pH-dependent zeta-potential analysis and found to be ~7 (Fig. S5). The SEC chromatogram reveals a bimodal molecular weight distribution with peak average molecular weights of ~7000 Da and 15 000 Da (overall average molecular weight: ~8800 Da), which is atypical of step-growth polymers (Fig. S6).

The morphology of the hyperbranched polymer in solution was studied using DLS and TEM analysis. The DLS CONTIN plot suggests that the number average diameter of PAE-TREN is ~10 nm (Fig. 2A). The TEM micrograph also supported this finding, as the average diameter was calculated to be 8 nm (Fig. 2B and C). These findings indicate that the hyperbranched polymer exists as ultrasmall molecular nanoparticles in solution.

The thermal properties of the polymer were studied using differential scanning calorimetry (DSC) and thermogravimetric analysis (TGA). The measured glass transition temperature (T_g) of PAE-TREN determined from differential scanning

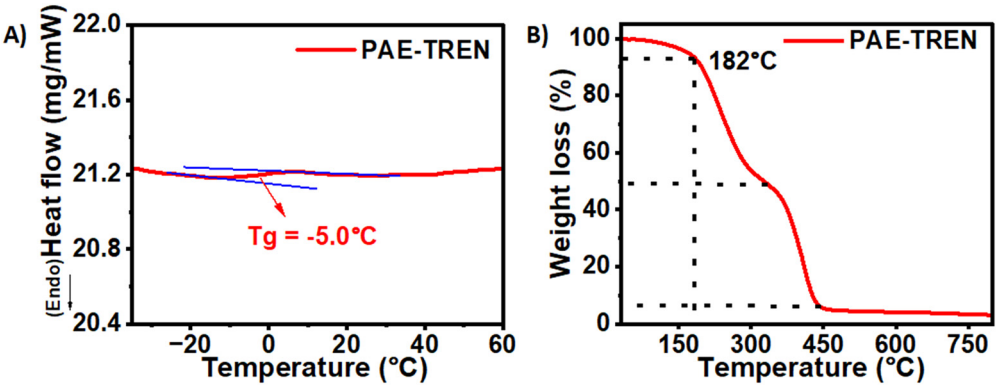

Fig. 3 Thermal characterizations. (A) DSC thermograph and (B) TGA of PAE-TREN.

calorimetry (DSC) was −5.0 °C (Fig. 3A). The TGA thermogram of PAE-TREN exhibits multistep thermal degradation, with thermal stability up to 182 °C (T_{d5}). Such multistep degradation is characteristic of the thermal degradation of poly(β-aminoester) backbones, in which the ester groups and the rest of the backbone undergo stepwise degradation (Fig. 3B).[48]

2.2. Temperature- and pH-responsive properties

The stimulus response behavior of the hyperbranched poly(β-aminoester) PAE-TREN was studied in detail. To test its temperature-dependent phase-transition behavior, the cloud point temperature (T_{cp}) of PAE-TREN was measured using UV-vis spectroscopy. Upon gradually increasing the temperature from 5 °C to 70 °C, a distinct phase transition was noted within the concentration range between 0.2 wt% to 1 wt%, with the transmittance (%) dropping sharply from ∼80% at 25 °C to <5% at 50 °C and the resulting solution turning cloudy (Fig. 4A, B and E). The T_{cp} was found to be 36 °C for 1 wt% polymer solution. To examine the reversibility of the thermo-responsiveness, the polymer solution was subjected to four consecutive heating–cooling cycles below and above the cloud point temperature at pH 7.0. The changes in the fluorescence intensity were recorded (Fig. S7), and the results clearly indicated that the polymer exhibits excellent reversible phase transition behavior for up to four complete cycles. These findings confirm the dynamic and reversible nature of the thermoresponsive property. Additionally, we also performed heating/cooling/heating cycles to examine the reversibility and possible hysteresis effect (Fig. S8). The cloud point temperature (T_{cp}) remained comparable (36 °C and 35 °C) during the first heating and second heating.

The presence of multiple tertiary amines in the PAE-TREN backbone enables protonation and makes it a pH-responsive polymer. To further understand the effect of pH on the critical temperature (T_{cp}), six solutions with varying pH values of pH 4.5, pH 5.5, pH 7.0, pH 8.1, pH 9.0 and pH 10.0 were tested (Fig. 4C). As the pH was increased from 7 to 9.0, the T_{cp} of PAE-TREN steadily increased. The recorded T_{cp} values were 36 °C,

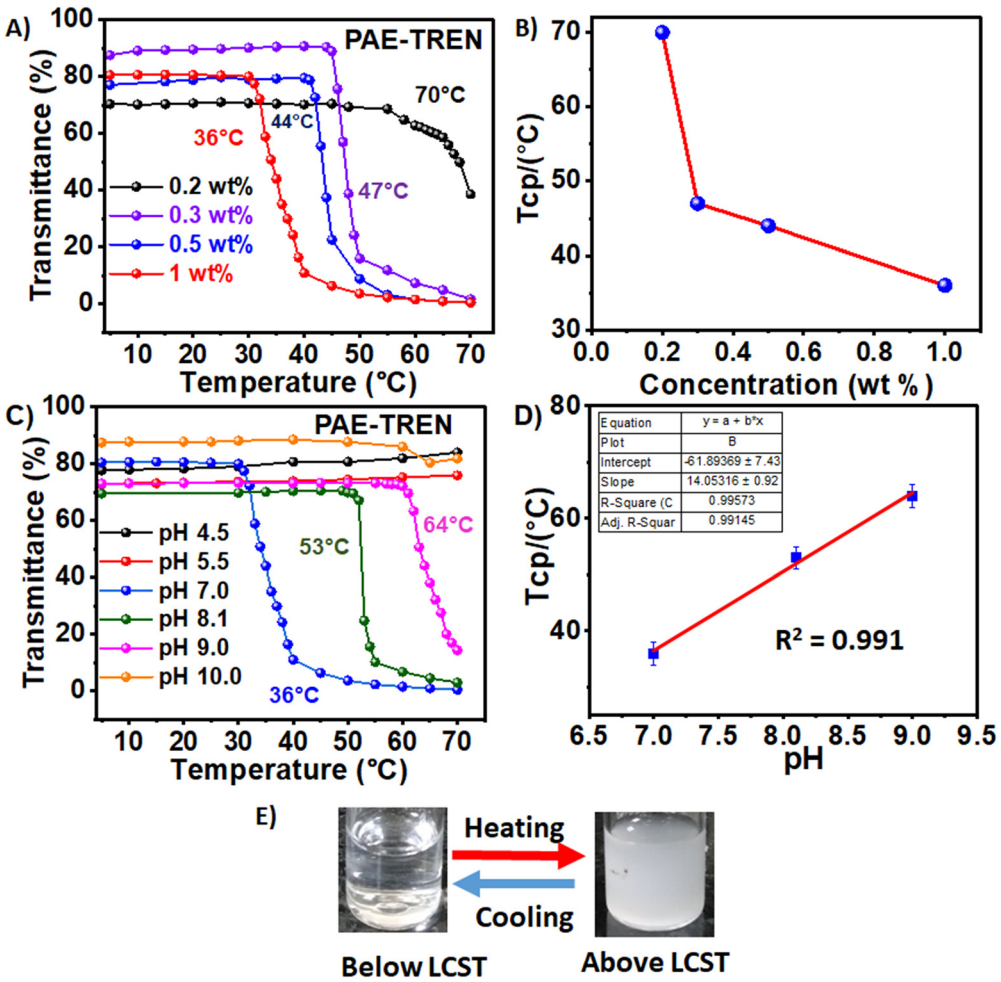

Fig. 4 (A) Temperature-dependent phase transition of PAE-TREN in solution at different concentrations (0.2 wt%, 0.3 wt%, 0.5 wt% and 1 wt%), (B) variation of the T_{cp} of PAE-TREN in solution (pH 7) at different concentrations. (C) Temperature-dependent phase transition of PAE-TREN (1 wt%) at different pH values (pH 4.5, pH 5.5, pH 7.0, pH 8.1, pH 9.0 and pH 10.0) (D) T_{cp} of PAE-TREN at different pH values. (E) Optical photograph of PAE-TREN in water below and above its T_{cp} (36 °C) at a concentration of 1 wt%.

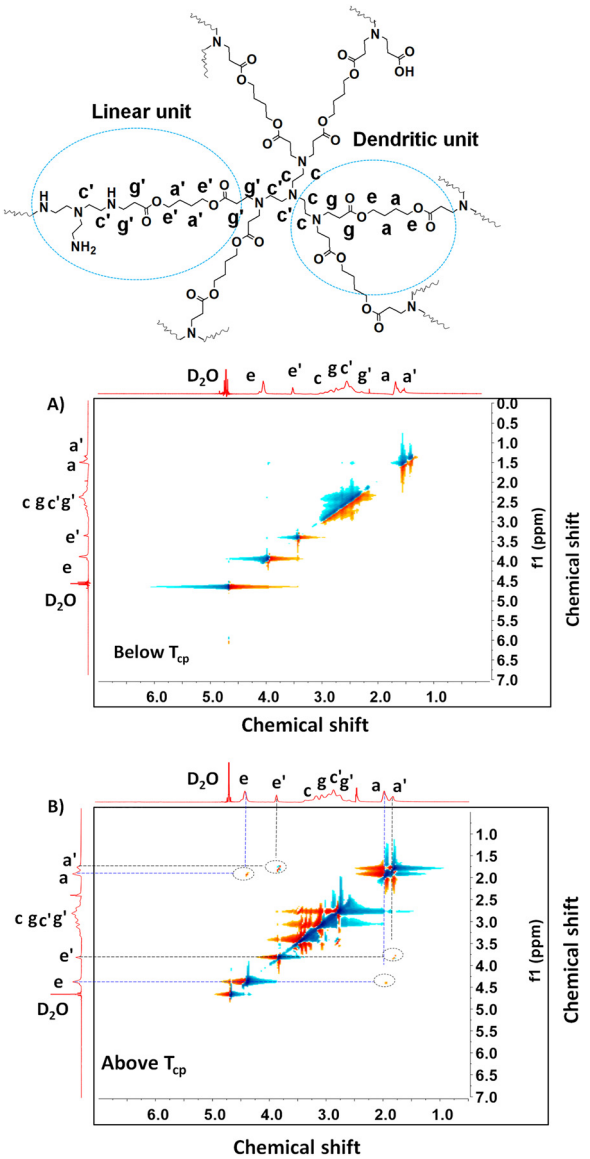

Fig. 5 (A) NOESY spectrum of PAE-TREN in D_2O at 20 °C (below its T_{cp} of ~36 °C) at a concentration of 1 wt%. (B) NOESY spectrum of PAE-TREN in D_2O at 60 °C (above its T_{cp} of ~36 °C) at a concentration of 1 wt%.

53 °C, and 64 °C at pH 7.0, 8.1, and 9.0, respectively (Fig. 4D). No phase transition was observed for PAE-TREN at lower pH (4.5 and 5.5) due to higher protonation of the amine groups, resulting in a highly hydrophilic backbone. Similarly, at pH 10.0, the formation of carboxylate ions at the terminal side of the hyperbranched polymer resulted in similar effects. The phase transition below and above T_{cp} indicates that PAE-TREN is more swollen (soluble) and forms a homogeneous solution in water through the formation of hydrogen bonds below T_{cp}, while above this temperature, the hydrogen bonds break and hydrophobic interactions increase, leading to further aggregation due to hydrophobic association driven by ester moieties within the backbone. The hydrophobic-association-driven phase separation below and above T_{cp} was further affirmed using nuclear overhauser effect spectroscopy (NOESY), which is an established method for proving molecular interactions and revealing phase transition behavior.[49] NOESY spectra of PAE-TREN were recorded both below (Fig. 5A) and above T_{cp} (Fig. 5B) for comparative study. The spectrum below T_{cp} (at 36 °C) did not exhibit any cross-peaks, which supported the absence of significant intra/intermolecular interactions. The presence of cross-peaks corresponding to hydrophobic interactions of ester moieties was observed above T_{cp} (at 60 °C) at 3.5 ppm and at 4.2 ppm (characteristic peaks of –OOC**CH$_2$CH$_2$CH$_2$CH$_2$**COO–) indicating local conformational crowding, suggesting hydrophobic association through molecular interaction and supporting the proposed origin of the temperature-responsive properties of PAE-TREN. It is important to note here that the choice of monomers such as 1,4-butanedioldiacrylate and tris-(2-aminoethylamine) (TREN) is crucial to the overall hydrophobic/hydrophilic balance and the formation of the temperature-responsive polymer. Replacing TREN with other monomers such as 1,4-butanediamine results in non-temperature-responsive polymers (results not included here). The dual-stimulus-responsive properties of hyperbranched PAE-TREN are compared with those of reported polymeric systems in Table S3.

2.3. Stimulus-defined photophysical properties for temperature and pH sensing

The absorption and fluorescence spectroscopy techniques were used to study the photophysical properties of the poly(β-aminoester) PAE-TREN. The absorption and excitation/emission spectra for PAE-TREN are presented in Fig. 6A. The current poly(β-aminoester) demonstrates an excitation peak at 360 nm and an absorption peak at 350 nm. Upon excitation at 360 nm, PAE-TREN exhibits maximum fluorescence intensity at 433 nm. The CIE 1931 chromaticity diagram of PAE-TREN shows the appearance of a blue color with (X, Y) coordinates of (0.15, 0.06) (Fig. 6B). Additionally, the quantum yield of PAE-TREN was calculated relative to quinine sulfate and found to be 16.0%, which is comparable to or better than those of other reported dendrimer-based fluorescent materials (Table S4). The nonconventional fluorescence properties of this non-conjugated hyperbranched poly(β-aminoester) can be attributed to the presence of electron-rich heteroatom functionalities, such as amines and esters, as well as the hyperbranched backbone, which promotes electron delocalization *via* through-space conjugation (TSC).[45,50]

Further studies were carried out to understand how the stimuli-responsive associative behavior influenced the photophysical properties, which would enable the detection of temperature and pH.

Temperature and pH are two crucial physiological parameters. In abnormal cells, the intracellular temperature is higher than 37 °C and may be ≥40 °C, and the pH is lower than 7.4, lying within the range of 5.5 to 6.8.[51–53] Therefore, determining these parameters is important to identify abnormal cells. The fluorescence emission of PAE-TREN in aqueous solution was studied by increasing the temperature from 10 °C to 70 °C (Fig. 7A). Fig. 7B illustrates the continuous linear

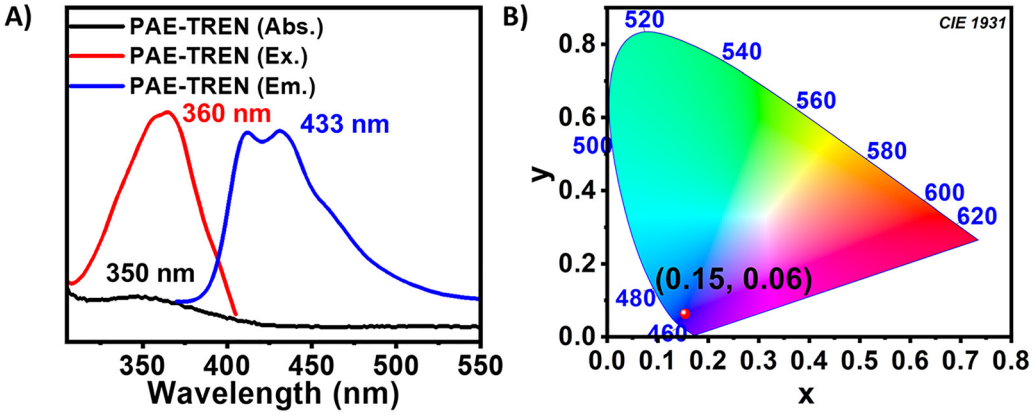

Fig. 6 (A) Excitation and emission spectra of PAE-TREN (0.1 wt%) with slit 2. (B) CIE 1931 chromaticity diagram of PAE-TREN (0.1 wt%) with slit 2.

decrease in fluorescence intensity observed within the physiological temperature range (30 °C to 42 °C). This occurs mainly because at higher temperatures, increased hydrophobic association (as demonstrated earlier) results in changes in the microenvironment, which likely disturb the existing through-space conjugation and facilitate increased non-radiative decay processes. To support the occurrence of non-radiative decay at higher temperature, fluorescence lifetime analysis was performed at a higher and lower temperature and revealed a small, but significant, decrease in the fluorescence lifetime at higher temperature, which was mainly attributed to increased non-radiative decay (Fig. S9A).

Similarly, the fluorescence emission of PAE-TREN was studied by increasing the pH from 5.2 to 8.3 (Fig. 7C). Fig. 7D exhibits a two-step linear decrease in fluorescence intensity, with different slopes below (from 5.5 to 6.8) and above (from 6.8 to 8.3) its isoelectric point (~7). The two different slopes are mainly due to the two different functional natures of the polymer, *i.e.*, above its isoelectric point, it acts as a cationic system, while below its isoelectric point, it acts as an anionic system. The increase in fluorescence intensity with decreasing pH can be attributed to the fact that protonation leads to a change in molecular geometry and electronic distribution, which may improve through-space conjugation. Lifetime analysis revealed a slightly longer lifetime at lower pH, which indicates decreased radiative decay and higher fluorescence intensity (Fig. S9B).

Overall, these findings demonstrate that PAE-TREN exhibits perfect linearity with both temperature as well as pH *via* a decrease in the fluorescence intensity of PAE-TREN. Hence, PAE-TREN can be used as a fluorescent nanoprobe for determining physiological temperature and pH.

To confirm the long-time hydrolytic stability of the polymer structure and its stimuli-dependent photophysical properties in solution, time-dependent analysis was performed for 380 h over 15 days. FTIR spectral analysis at different time intervals affirmed that the chemical structure of the polymer remained intact in solution without any chemical change/degradation (Fig. S10). In addition to this, DLS study of PAE-TREN over time (for ~380 h) at pH values of 5.5, 7.0 and 9.0 (temperature 37 °C) confirmed the stability of PAE-TREN. At pH 5.5, the size of PAE-TREN was ~32.0 nm, while its size was ~12.0 nm and ~5 nm at pH 7.0 and 9.0 through 380 h (Fig. S11–S13). Additionally, to understand the retention of the photophysical properties of PAE-TREN, kinetic studies *via* fluorescence intensity measurement over ~380 h were performed at pH 5.5, pH 7.0 and pH 9.0 (Fig. S14). No significant decrease in the fluorescence intensity was observed. This indicates that PAE-TREN is sufficiently stable under acidic and basic conditions. These outcomes confirm the excellent hydrolytic stability of PAE-TREN at pH 5.5, pH 7.0 and pH 9.0 for a significantly long time.

2.4. Controlled drug delivery using the poly(β-aminoester)

Typically, dendrimers and hyperbranched polymers are used for drug encapsulation and delivery. The hyperbranched molecular architecture and stimuli-responsive properties of PAE-TREN inspired us to investigate its potential for controlled drug delivery. For an *in vitro* study, methylene blue was used as a model drug[54,55] due to its affordability, easy detection by standard UV-vis spectroscopy, low toxicity, ability to cross the blood–brain barrier,[56–59] and its potential application in various neurological conditions, making it one of the WHO-listed essential medicines.[60] The hyperbranched geometry of the poly(β-aminoester) PAE-TREN facilitated the incorporation of methylene blue (as a model drug) into the hyperbranched PAE-TREN backbone in acetone at room temperature. In this type of encapsulation approach, drug molecules are generally loaded within the intramolecular cavities of the hyperbranched polymer chains.[61] Thereby, the pH- and temperature-responsive changes within the intramolecular cavities are expected to influence the drug release. Its encapsulation efficiency was quantified and found to be very high, with a calculated drug loading efficiency of 99%.

The controlled release behavior of the encapsulated methylene blue (MB) was analyzed using UV-visible spectroscopy. pH-dependent release studies were conducted in buffer solutions with pH values of 5.5, 7.0 and 9.0 to evaluate the influence of pH at a constant temperature of 37 °C (Fig. 8A). For the poly(β-aminoester) PAE-TREN, MB release was slightly faster at pH 9.0 compared to pH 7.0 and then pH 5.5 during the initial

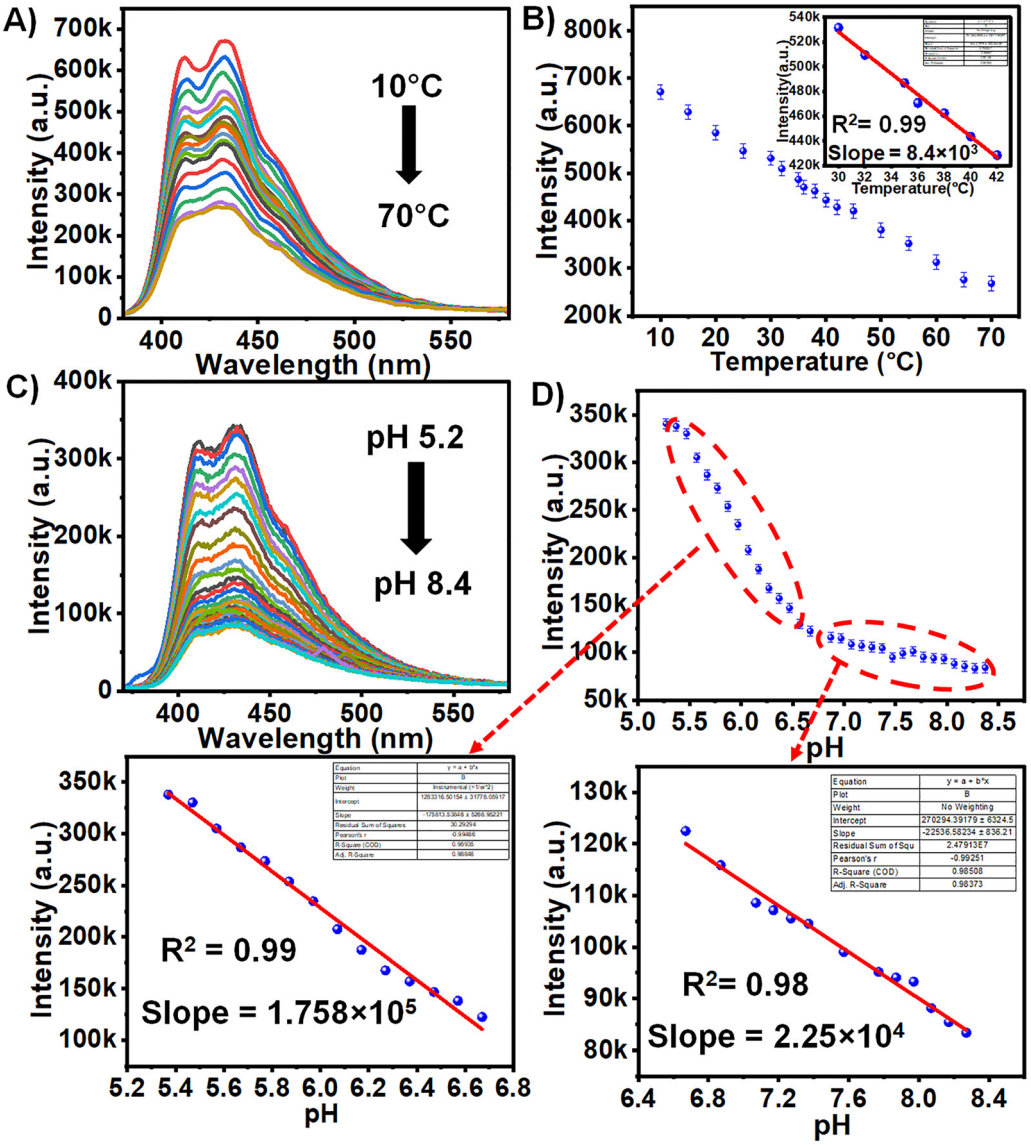

Fig. 7 (A) Fluorescence emission spectra of PAE-TREN (1 wt%) at temperatures from 5 °C to 70 °C. (B) Variation of fluorescence intensity with respect to temperature from 5 °C to 70 °C. (C) Fluorescence emission spectra of PAE-TREN (1 wt%) at pH values from 5.2 to pH 8.3. (D) Variation of fluorescence intensity with respect to the pH from pH 5.2 to pH 8.3, along with expansions of the plots showing their linearity below and above pH 6.8.

24 h. A slow release of MB was observed at pH 5.5 for approximately 30 h. However, PAE-TREN showed approximately 75% MB release at pH 7.0. Similarly, the influence of the temperature on the methylene blue (MB) release behavior of PAE-TREN was analyzed using UV-visible spectroscopy. Release kinetics were studied at three different temperatures, namely, 25 °C, 37 °C and 60 °C, to evaluate the influence of temperature; the pH was maintained at 7.0 (Fig. 8B). For the poly-(β-aminoester) PAE-TREN, an initial burst of MB release was observed at both 25 °C and 60 °C. Conversely, a sustained MB release was observed at 37 °C during the initial 20 h compared to the other temperatures. Overall, the most sustained and efficient drug release was observed under physiological conditions at a temperature of 37 °C and pH 7. This stimulus-responsive delivery of such systems can be explained, as below the LCST, the intramolecular cavities of the hyperbranched polymer chains do not undergo any change, making the drug release less efficient. Above the LCST, the hyperbranched polymer nanoparticles collapse, leading to a significant reduction in intramolecular cavity size and, consequently, a burst release of the drug is observed. At the phase-transition temperature, however, an optimal balance between these effects enables the most sustained release.

To support this explanation, we performed DLS measurements of MB-loaded PAE-TREN at three different temperatures (25 °C, 37 °C and 60 °C). At 25 °C, the size of the MB-loaded PAE-TREN is 32 nm, while it is 15 nm and 3 nm at 37 °C and 60 °C, respectively (Fig. S15). These results strongly support the conclusion that the release kinetics are governed by the temperature-dependent cavity size of the polymer. Above the

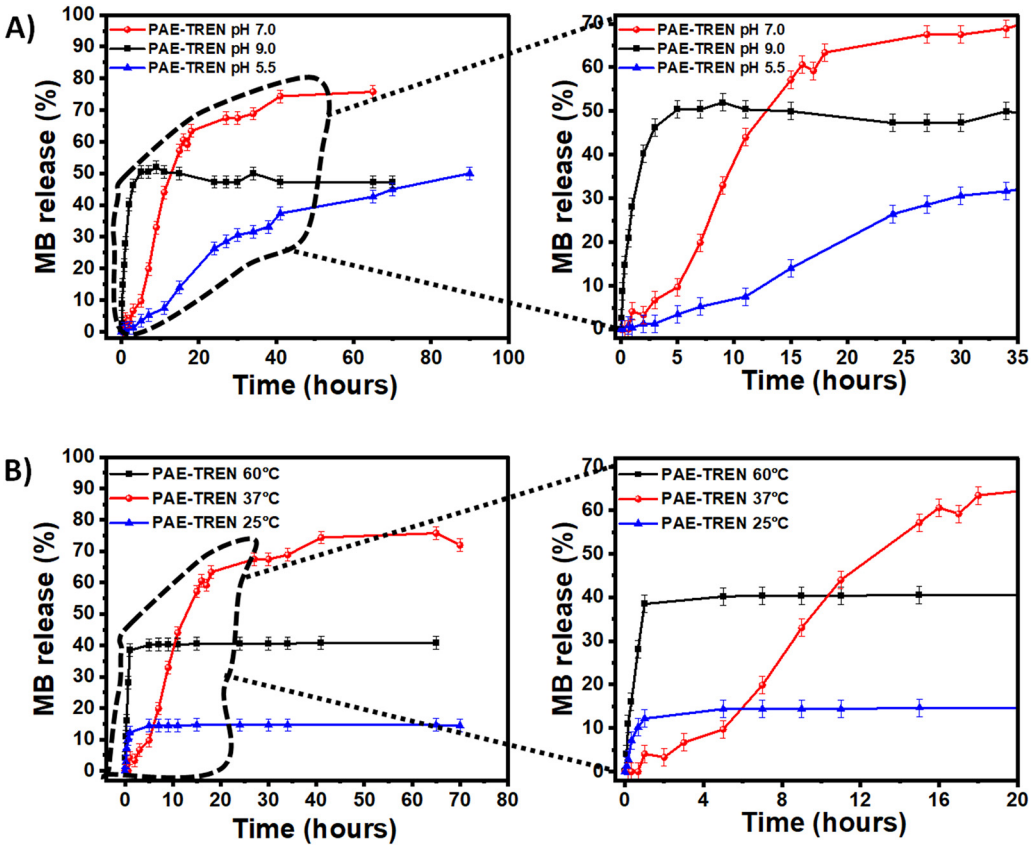

Fig. 8 (A) pH-Dependent release kinetics of MB from PAE-TREN at a temperature of 37 °C, along with an expanded view of the lower region of the plot. (B) Temperature-dependent release kinetics of MB from PAE-TREN at pH 7.0, along with an expanded view of the lower region of the plot.

CPT (cloud point temperature), the collapse reduces free volume and expels entrapped drug molecules, leading to burst release. Below the CPT, the swollen state provides larger cavities that retain the drug more effectively.

Additionally, at pH 9, the size of MB-loaded poly(β-aminoester) is 7 nm, while it is 15 nm and 38 nm at pH 7 and 5.5, respectively (Fig. S16). At pH 9, the polymer structure is highly compact due to the deprotonation of tertiary amines. This collapse reduces the internal cavity volume, which leads to rapid removal of physically entrapped MB at the alkaline pH of 9 (burst release). At lower pH values, the polymer is more swollen with larger cavities, allowing MB molecules to be retained longer through a combination of steric confinement and weak interactions.

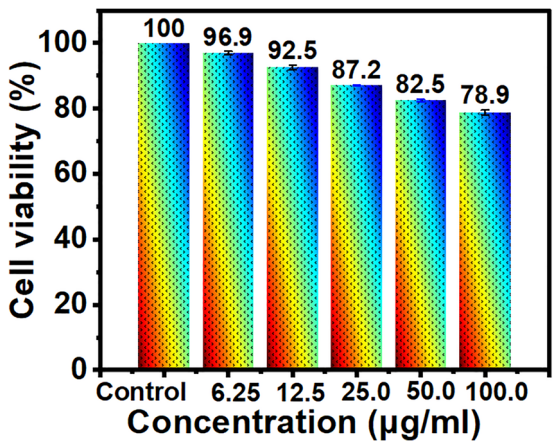

Fig. 9 L929 cell viability after 24 h of incubation with PAE-TREN with increasing concentration: 6.25 μg mL^{-1}, 12.5 μg mL^{-1}, 25.0 μg mL^{-1}, 50.0 μg mL^{-1} and 100.0 μg mL^{-1}.

2.5. Cytotoxicity test

To evaluate the biocompatibility of the poly(β-aminoester) PAE-TREN for practical use, an MTT assay was conducted using L929 cells (mouse fibroblast cells). The hyperbranched poly(β-aminoester) is biocompatible at a concentration of 100 μg mL^{-1}, with a cell viability above 75%. At lower concentrations, the polymer shows negligible cytotoxicity; specifically, up to 12.5 μg mL^{-1}, >90% cell viability was observed (Fig. 9). Additionally, the LC_{50} value of PAE-TREN was determined to be 304.446 μg mL^{-1}. Overall, these findings suggest that the newly synthesized PAE-TREN is biocompatible for potential future *in vivo* applications.

3. Conclusions

In summary, we developed a sustainable one pot synthetic strategy to prepare the hyperbranched β-polyaminoester

PAE-TREN containing zwitterionic branch ends (amine and acid groups) using aza-Michael polyaddition reactions between 1,4-butanedioldiacrylate and tris-(2-aminoethylamine) (TREN) in water at room temperature. The molecular structure of the polymer was characterized using NMR and FTIR, which revealed a hyperbranched architecture with a calculated degree of branching of 75%. DLS and TEM reveal that in solution, the polymer exists as ultrasmall nanoparticles with an average hydrodynamic diameter of ~10 nm. Thermal analysis using TGA and DSC confirms that the polymer is stable up to 182 °C (T_{d5}) and has a glass transition temperature of −5 °C. The isoelectric point of the polymer was determined to be pH ~7. The polymer exhibits pH-dependent thermoresponsive properties with a cloud point temperature (T_{cp}) of 36 °C at pH ~7. The temperature-responsive associative behavior of the polymer can be ascribed to the hydrophobic association of the ester segments at higher temperatures, as supported by NOESY NMR analysis. The polymer exhibits blue emission with a quantum yield of 16%. Further, the temperature- and pH-dependent associative behaviors of the polymer influence its photophysical properties, with linear relations being observed, thus enabling its effective use as a nanosensor to measure physiological temperature and pH. A model *in vitro* drug release study supports its effective use in the context of sustained and controlled delivery up to 20 h under physiological temperature and pH (37 °C and pH ~7). MTT assay reveals that the polymer is biocompatible for practical applications.

Author contributions

SG: design of experiments, synthesis, characterization, application, relevant data analysis, (lead), writing (lead), AA: characterization (supporting), witting (supporting) SC: conceptualization of the actual work and supervision, writing (lead and review). All the authors have approved the final manuscript.

Conflicts of interest

There are no conflicts to declare.

Data availability

The data supporting this article have been included as part of the supplementary information (SI). Supplementary information: all the experimental details and characterization details are given in supporting information. See DOI: **https://doi.org/10.1039/d5sm00635j**.

Acknowledgements

SG and AA acknowledge IIT Patna for the research fellowship. SAIF, IIT Patna is acknowledged for the DLS, TGA, DSC and zeta-potential analysis.

References

1 J. Liu, H. Guo, Q. Gao, H. Li, Z. An and W. Zhang, *Macromolecules*, 2022, **55**, 8524–8532.
2 S. Ghosh, M. Avais and S. Chattopadhyay, *Chem. Commun.*, 2022, **58**, 12807–12810.
3 P. Zhao, J. Xia, M. Cao and H. Xu, *ACS Macro Lett.*, 2020, **9**, 163–168.
4 J. A. McCune, S. Mommer, C. C. Parkins and O. A. Scherman, *Adv. Mater.*, 2020, **32**, 1906890.
5 S. Mommer and S. J. Wezenberg, *ACS Appl. Mater. Interfaces*, 2022, **14**, 43711–43718.
6 X. Liu, Y. Yang and M. W. Urban, *Macromol. Rapid Commun.*, 2017, **38**, 1700030.
7 F. Yelda Ünlü and A. Aydogan, *Macromol. Rapid Commun.*, 2022, **43**, 2200447.
8 C. Zhang, G. Ye, W. Wang, X. Ding, Y. Feng and R. Wang, *ACS Appl. Nano Mater.*, 2024, **7**, 370–381.
9 B. Iyisan, R. Thiramanas, N. Nazarova, Y. Avlasevich, V. Mailänder, S. Baluschev and K. Landfester, *Biomacromolecules*, 2020, **21**, 4469–4478.
10 D. Datta, V. Colaco, S. P. Bandi, N. Dhas, L. S. L. Janardhanam, S. Singh and L. K. Vora, *ACS Biomater. Sci. Eng.*, 2025, **11**(3), 1338–1372.
11 N. Das, T. Samanta, D. Patra, P. Kumar and R. Shunmugam, *Macromol*, 2024, **57**, 976–984.
12 S. Kumari, M. Avais and S. Chattopadhyay, *ACS Appl. Polym. Mater.*, 2023, **5**, 1626–1645.
13 M. Sahn, T. Yildirim, M. Dirauf, C. Weber, P. Sungur, S. Hoeppener and U. S. Schubert, *Macromolecules*, 2016, **49**, 7257–7267.
14 P. J. Roth, T. P. Davis and A. B. Lowe, *Macromolecules*, 2012, **45**, 3221–3230.
15 L. Mäkinen, D. Varadharajan, H. Tenhu and S. Hietala, *Macromolecules*, 2016, **49**, 986–993.
16 P. Freeman and J. Rowlinson, *Polymer*, 1960, **1**, 20–26.
17 P. Srikamut, T. Phakkeeree, F. Seidi, S. Iamsaard and D. Crespy, *ACS Appl. Polym. Mater.*, 2021, **3**, 5425–5433.
18 G. Yang, J. Wang, Y. Yan, Z. Hai, Z. Hua and G. Chen, *Biomacromolecules*, 2020, **21**, 4159–4168.
19 X. Liu, D. Hu, Z. Jiang, J. Zhuang, Y. Xu, X. Guo and S. Thayumanavan, *Macromolecules*, 2016, **49**, 6186–6192.
20 Y. Li, J. Luo, G. Xie, D. Zhu, C. Zhao, X. Zhang, M. Liu, Y. Wu, Y. Guo and W. Yu, *ACS Appl. Polym. Mater.*, 2024, **7**, 1–11.
21 F. Termühlen, D. Kuckling and M. Schönhoff, *J. Phys. Chem. B.*, 2017, **121**, 8611–8618.
22 F. Yin, P. Laborie, B. Lonetti, S. Gineste, Y. Coppel, N. Lauth-de Viguerie and J.-D. Marty, *Macromolecules*, 2023, **56**, 3703–3720.
23 S. Vandewalle, M. Van De Walle, S. Chattopadhyay and F. Du Prez, *Eur. Polym. J.*, 2018, **98**, 468–474.
24 S. Pal, M. R. Hill and B. S. Sumerlin, *Polym. Chem.*, 2015, **6**, 7871–7880.
25 S. Vandewalle, S. Wallyn, S. Chattopadhyay, C. R. Becer and F. Du Prez, *Eur. Polym. J.*, 2015, **69**, 490–498.

26 S. Laroque, K. E. S. Locock and S. Perrier, *Biomacromolecules*, 2025, **26**, 190–200.
27 L. Wang, F. Liu, J. Qian, Z. Wu and R. Xiao, *Soft Matter*, 2021, **17**, 10421–10427.
28 X. Li, Y. Wang, D. Li, M. Shu, L. Shang, M. Xia and Y. Huang, *Soft Matter*, 2021, **17**, 6688–6696.
29 K. Kolouchová, V. Lobaz, H. Beneš, V. R. de la Rosa, D. Babuka, P. Švec, P. Černoch, M. Hrubý, R. Hoogenboom and P. Štěpánek, *Polym. Chem.*, 2021, **12**, 5077–5084.
30 O. Sedlacek, D. Bera and R. Hoogenboom, *Polym. Chem.*, 2019, **10**, 4683–4689.
31 K. Yamamoto, T. Serizawa, Y. Muraoka and M. Akashi, *Macromolecules*, 2001, **34**, 8014–8020.
32 R. Kanno, M. Ouchi and T. Terashima, *Polym. Chem.*, 2023, **14**, 1718–1726.
33 S. Chattopadhyay, E. Heine, A. Mourran, W. Richtering, H. Keul and M. Möller, *Polym. Chem.*, 2016, **7**, 364–369.
34 X. Wang, Z. Zhang and N. Hadjichristidis, *Prog. Polym. Sci.*, 2023, **136**, 101634.
35 J. P. Swanson, M. A. Cruz, L. R. Monteleone, M. R. Martinez, P. J. Costanzo and A. Joy, *Polym. Chem.*, 2017, **8**, 7195–7206.
36 T. R. Blake and R. M. Waymouth, *J. Am. Chem. Soc.*, 2014, **136**, 9252–9255.
37 D. Zhou, L. Pierucci, Y. Gao, J. O'Keeffe Ahern, X. Huang, A. Sigen and W. Wang, *ACS Appl. Mater. Interfaces*, 2017, **9**, 5793–5802.
38 W. Cheng, D. Wu and Y. Liu, *Biomacromolecules*, 2016, **17**, 3115–3126.
39 X.-Y. Liu, X.-R. Mu, Y. Liu, H.-J. Liu, Y. Chen, F. Cheng and S.-C. Jiang, *Langmuir*, 2012, **28**, 4867–4876.
40 B. Wang, T. Xiao, X.-B. Fu, T.-T. Jiang, Y. Chen and Y.-F. Yao, *Macromolecules*, 2017, **50**, 9647–9655.
41 J. Zhang, H.-J. Liu, Y. Yuan, S. Jiang, Y. Yao and Y. Chen, *ACS Macro Lett.*, 2013, **2**, 67–71.
42 D. Jaworska-Krych, M. Gosecka, P. Maczugowska, K. Hałagan, K. Szutkowski, M. Gosecki, M. Urbaniak and M. Kozanecki, *Macromolecules*, 2024, **57**, 9135–9156.
43 L. Sun, F. Gao, D. Shen, Z. Liu, Y. Yao and S. Lin, *Polym. Chem.*, 2018, **9**, 2977–2983.
44 Z. Jia, H. Chen, X. Zhu and D. Yan, *J. Am. Chem. Soc.*, 2006, **128**, 8144–8145.
45 Y. Du, T. Bai, H. Yan, Y. Zhao, W. Feng and W. Li, *Polymer*, 2019, **185**, 121771.
46 L. J. Markoski, J. L. Thompson and J. S. Moore, *Macromolecules*, 2002, **35**, 1599–1603.
47 J.-J. Max and C. Chapados, *J. Phys. Chem. A*, 2004, **108**, 3324–3337.
48 H. Mahdavi, A. Kamyabi, T. Shahalizade and H. Asadollahi Taheri, *Cellulose*, 2017, **24**, 5389–5402.
49 A. T. Hendricksen, S. Ezzatpour, A. J. Pulukuri, A. T. Ryan, T. J. Flanagan, W. Frantz, D. W. Buchholz, V. Ortega, I. A. Monreal and J. M. Sahler, *Adv. Healthcare Mater.*, 2023, **12**, 2202918.
50 L. Yuan, H. Yan, L. Bai, T. Bai, Y. Zhao, L. Wang and Y. Feng, *Macromol. Rapid Commun.*, 2019, **40**, 1800658.
51 T. Volk, E. Jähde, H. Fortmeyer, K. Glüsenkamp and M. Rajewsky, *Br. J. Cancer*, 1993, **68**, 492–500.
52 R. D. Issels, *Eur. J. Cancer*, 2008, **44**, 2546–2554.
53 Z. Ge and S. Liu, *Chem. Soc. Rev.*, 2013, **42**, 7289–7325.
54 A. Miclescu and L. Wiklund, *J. Rom. Anest. Terap. Int.*, 2010, **17**, 35–41.
55 T. P. Pivetta, Q. Ferreira, T. Vieira, J. C. Silva, S. Simões, P. A. Ribeiro and M. Raposo, *Colloids Surf., B*, 2022, **220**, 112901.
56 H. Xue, A. Thaivalappil and K. Cao, *Cells*, 2021, **10**, 3379.
57 J. C. Rojas, A. K. Bruchey and F. Gonzalez-Lima, *Prog. Neurobiol.*, 2012, **96**, 32–45.
58 P. R. Ginimuge and S. Jyothi, *J. Anaesthesiol., Clin. Pharmacol.*, 2010, **26**, 517–520.
59 I. Jack Clifton and J. B. Leikin, *Am. J. Ther.*, 2003, **10**, 289–291.
60 *World Health Organization, World Health Organization model list of essential medicines: 21st list 2019*, World Health Organization, Geneva, 2019.
61 Q. Ban, W. Sun, J. Kong and S. Wu, *Chem. – Asian J.*, 2018, **13**, 3341–3350.

